Article ID: 1006-8775(2021) 04-0428-09

An Innovative Bias-Correction Approach to CMA-GD Hourly Quantitative Precipitation Forecasts

LIU Jin-qing (刘金卿)[1, 2, 3, 4], DAI Guang-feng (戴光丰)[2], OU Xiao-feng (欧小锋)[1, 4]
(1. Hunan Meteorological Observatory, Changsha 410118 China; 2. Guangzhou Institute of Tropical and Marine Meteorology/ Guangdong Provincial Key Laboratory of Regional Numerical Weather Prediction, CMA, Guangzhou 510640 China; 3. Heavy Rain and Drought Flood Disasters in Plateau and Basin Key Laboratory of Sichuan, Chengdu 610072 China; 4. Hunan Key Laboratory of Meteorological Disaster Prevention and Reduction, Changsha 410118 China)

Abstract: This paper proposes a simple and powerful optimal integration (OPI) method for improving hourly quantitative precipitation forecasts (QPFs, 0-24 h) of a single-model by integrating the benefits of different bias-corrected methods using the high-resolution CMA-GD model from the Guangzhou Institute of Tropical and Marine Meteorology of China Meteorological Administration (CMA). Three techniques are used to generate multi-method calibrated members for OPI: deep neural network (DNN), frequency-matching (FM), and optimal threat score (OTS). The results are as follows: (1) The QPF using DNN follows the basic physical patterns of CMA-GD. Despite providing superior improvements for clear-rainy and weak precipitation, DNN cannot improve the predictions for severe precipitation, while OTS can significantly strengthen these predictions. As a result, DNN and OTS are the optimal members to be incorporated into OPI. (2) Our new approach achieves state-of-the-art performances on a single model for all magnitudes of precipitation. Compared with the CMA-GD, OPI improves the TS by 2.5%, 5.4%, 7.8%, 8.3%, and 6.1% for QPFs from clear-rainy to rainstorms in the verification dataset. Moreover, OPI shows good stability in the test dataset. (3) It is also noted that the rainstorm pattern of OPI relies heavily on the original model and that OPI cannot correct for deviations in the location of severe precipitation. Therefore, improvements in predicting severe precipitation using this method should be further realized by improving the numerical model's forecasting capability.

Key words: DNN; deep-learning; bias-correction; post-processing; OTS; optimal integration; NWP
CLC number: P456.7 **Document code:** A
Citation: LIU Jin-qing, DAI Guang-feng and OU Xiao-feng. An Innovative Bias-Correction Approach to CMA-GD Hourly Quantitative Precipitation Forecasts [J]. Journal of Tropical Meteorology, 2021, 27(4): 428-436, https://doi.org/10.46267/j.1006-8775.2021.037.

1 INTRODUCTION

Numerical weather prediction (NWP) is not always accurate in rainfall prediction (Bauer et al. [1]; Leutbecher et al. [2]; Dias et al. [3]; Xue and Liu [4]; Subramanian et al. [5]; Zhang et al. [6]). One effective method of improving the accuracy of NWP is to correct the deviation of the forecast from the observation based on statistical corrective methods (Bentzien and Friederichs [7]; Volosciuk et al. [8]; Mendez et al. [9]). For example, Zhu and Luo [10] demonstrated that the frequency-matching (FM) method can significantly reduce the systematic bias of precipitation intensity. Hamill et al. [11] pointed out that an analog post-processing method based on historically similar weather system can effectively correct the spatial distribution of precipitation. In addition, meteorologists also pay attention to extracting effective information from ensemble forecasts or multi-model forecasts and to generating deterministic quantitative precipitation forecasts (QPF) with higher accuracy (Woodcock and Engel [12]; Tartaglione et al. [13]; Ebert et al. [14]; Kumar et al. [15]; Sukovich et al. [16]). For example, Dai et al. [17] contended that the optimal percentage method could integrate effective information with different percentiles, while the probability-matching (PM) method could acquire a better spatial distribution field from multi-models (Ebert [18]), especially the weighted PM (WPM) method, which could automatically give a very low weight to the less skillful model (Liu et al. [19]).

Another approach to improving QPF is to develop better weather predicting models by interpreting high-resolution NWP outputs (Gagne et al. [20]; Rasp and Lerch [21]; Herman and Schumacher [22]; Zhou et al. [23]; Chattopadhyay et al. [24]; Xia et al. [25]; Han et al. [26]).

Received 2021-08-26 **Revised** 2021-09-15 **Accepted** 2021-11-15
Funding: Open Project Fund of Guangdong Provincial Key Laboratory of Regional Numerical Weather Prediction, CMA (J202009); Heavy Rain and Drought-Flood Disasters in Plateau and Basin Key Laboratory of Sichuan Province (SZKT202005); Innovation and Development Project of China Meteorological Administration (CXFZ2021J020)
Biography: LIU Jin-qing, PhD., primarily undertaking research on mechanism and forecast of rainstorms.
Corresponding author: LIU Jin-qing, e-mail: liujq_0912@126.com

More recently, deep learning (DL) algorithms have been explosively applied in weather forecasts and have proven successful in difficult rainfall classification tasks (Nagaselvi and Deepa [27]; Reichstein et al. [28]; Chen et al. [29]). For instance, Yuan et al. [30] pointed out that the artificial neural network (ANN) showed good performance in adjusting for high-resolution probabilistic QPF outputs. Scher and Messori [31] suggested that the convolutional neural network (CNN) could be useful for quantifying the uncertainty of NWP. Zhang et al. [32] proposed a prediction model combining *k*-means clustering and CNN to improve short-term rainfall forecasting.

However, due to the highly nonlinear and stochastic nature of the temporal-spatial distribution of precipitation, the above methods have some limitations. Statistical corrective methods cannot overcome major model errors (Maraun et al. [33]). Although the DL method has limited modeling capacity for small-sample events (e. g., short-term rainstorms), it can use big data relationships to create a better classification forecast model for big-sample events (e. g., weak rain). As a result, problems in integrating different bias-corrected technologies have several unique challenges, requiring methodologies converting precipitation classifications to QPF and combining the benefits of various methods.

This paper introduces a simple but powerful approach for overcoming these existing challenges based on CMA-GD model from the Guangzhou Institute of Tropical and Marine Meteorology of China Meteorological Administration (CMA). CMA officially approved the CMA-GD model for service operation in 2011 (Zhong and Chen. [34]; Zhong et al. [35]). The rest of this article is organized as follows. Section 2 provides an overview of data and methodology. Section 3 discusses the results of the new approach. Section 4 gives case studies of successes and failures. Section 5 provides concluding remarks by briefly discussing the effectiveness and limitations of this approach.

2 DATA AND METHODOLOGY

2.1 *Data*

The high-resolution (3 km, hourly) products of CMA-GD model (Fig. 1) were used in this paper from January 2018 to March 2021, with the initial times at 00:00 and 12:00 UTC and a valid forecast period of 0-24 h. The grid data were the nearest neighbor interpolated to 420 stations in Hunan Province (24−31°N, 108−115 °E) in order to be consistent with observations. Moreover, the observational data was provided by the China Integrated Meteorological Information Sharing System (CIMISS) (Sun et al. [36]).

Data division: All samples were divided into a training dataset, verification dataset, and test dataset (Table 1), with the verification set used to determine the integration solution and the test set used as an independent sample for forecasting. According to CMA's service requirements for short-time precipitation (T/CMSA 0013−2019), the hourly rainfall was divided into six grades at thresholds of 0.1, 2, 4, 8, and 20 mm h^{-1}. Here a clear day occurred when the per-hour rainfall was less than 0.1 mm h^{-1}, since 0.1 mm is the smallest detectable amount of rain gauge in China. And rainstorms occurred when the per-hour rainfall exceeded 8 mm h^{-1}. Since the number of small-scale samples (<4 mm) in the training set was greatly imbalance from that of the large-scale samples, the small-scale samples were under-sampled at a ratio of 1: 10, and the number of samples at each scale is ten times that of the severe rainstorm samples to obtain balanced samples.

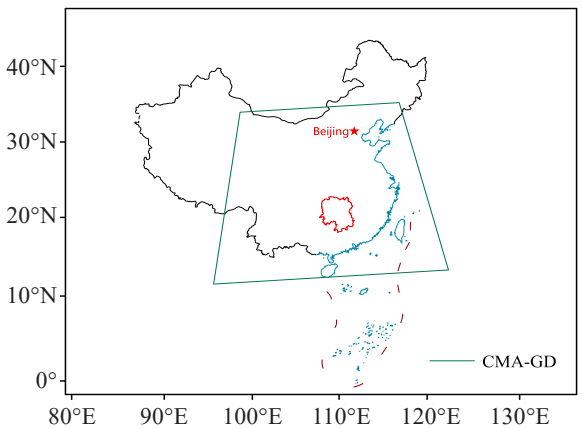

Figure 1. Domain of the CMA-GD model in Lambert map projection. The red line represents the location of Hunan Province.

2.2 *Method*

2.2.1 GENERATING MULTI-METHOD CALIBRATED MEMBERS

Three techniques were used in this step to build the QPF correction models (Table 2), including deep neural network (DNN), frequency-matching (FM) and optimal threat score (OTS). Among them, the DNN technique aims to reduce the location and magnitude biases of rainfall. While FM and OTS can only eliminate the deviation in magnitude between QPF and the observation, they are unable to correct for pattern biases (Zhu and Luo [10]; Wu et al. [37]; Wu and Chen[38]). The thresholds of FM and OTS are 0.1, 2, 4, 8, and 20 mm.

For DNN, the training set was used to obtain the classification of precipitation grades consistent with Table 1, and verification was performed with the verification set. Throughout the whole training process, DNN maintained the model with highest accuracy of classification in the verification set.

Hyperparameters: The Adam optimizer (Kingma and Ba [39]), cross-entropy loss function, and StepLR scheduler were used. The learning rate was set at 0.001 initially and was updated with the optimizer and scheduler. Batch normalization was used (Ioffe and

Table 1. Sample sizes for the different grades of datasets from January 2018 to March 2021 (units: number).

Datasets	Period	<0.1	0.1≤x < 2	2≤x < 4	4≤x < 8	8≤x < 20	>=20
Training (original)	2018.1—2019.12	11869522	1495536	143606	75625	36572	8114
Training (sampling)	2018.1—2019.12	81140	81140	81140	75625	36572	8114
Validation	2020.1—2021.3 random 50%	3416554	457119	49399	24087	10278	2107
Test	2020.1—2021.3 rest 50%	3352259	511314	56631	25761	11011	2332

Table 2. List of different techniques for improving quantitative precipitation forecast.

Method	Principle	Effect	Training window
Deep neural network (DNN)	Hinton [41]	Predict classification of QPF	2018.1−2019.12
Frequency-matching (FM)	Zhu and Luo [10]	Adjust magnitude of QPF	Past 30 days of the same year and the next 30 days of last year
Optimal threat score (OTS)	Wu et al. [37]	Same as FM	Same as FM

Szegedy [40]). The number of epochs was set at 200. All of the stations were used here for unified modeling.

Selection of variables: From different levels and types of physical variables in CMA-GD, 51 physical variables (Table 3) related to precipitation and severe convection were selected. All variables were normalized to eliminate the dimensional difference between different variables before training.

Table 3. Physical variables used in DNN.

Feature	Description
Rain	Hourly precipitation
CAPE	Convective available potential energy
CIN	Convective inhibition
K	K index
SI	Showalter index
IVT	Integrated vapor transport
IVTD	Divergence of IVT
U10/V10	10-meter U-wind and V-wind
T2/Rh2	2-meter temperature and relative humidity
Theta	Equivalent potential temperature at 500/700/850/925/1000 hPa
W	Vertical velocity at 500/700/850/925/1000 hPa
GH	Geopotential height at 500/700/850/925/1000 hPa
DIV/VOR	Divergence and vorticity at 500/700/850/925/1000 hPa
T/Td	Temperature and dew point temperature at 500/700/850/925/1000 hPa
Vapor	Vapor flux at 500/700/850/925/1000 hPa

Mapping: To conduct a quantitative comparison with FM and OTS technologies, the DNN classification results should be transformed into QPF. The linearly mapping method from forecast probability to QPF was used here (Fig. 2). The rainfall is calculated as follows:

$$y = \begin{cases} 0, \ k < 1 \\ \mathrm{OBS}_k + \left(\mathrm{OBS}_{k+1} - \mathrm{OBS}_k\right)\dfrac{x_k - P_{\min}}{P_{\max} - P_{\min}}, \ k \in \{1,2,3,4\} \\ \mathrm{OBS}_5 + \dfrac{x_k - P_{\min}}{P_{\min}} \times \mathrm{OBS}_5, \ k \geqslant 5 \end{cases}$$

where x and y are the forecast probability and QPF for different precipitation grades, respectively; OBS_k is the kth precipitation threshold, which is consistent with the thresholds of FM and OTS (0.1, 2, 4, 8, and 20); and P is the forecast probability set of different magnitudes for the calculated training dataset and validation dataset.

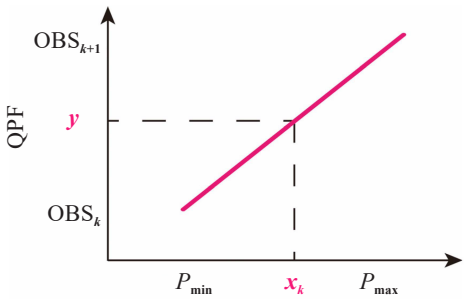

Figure 2. Illustration of the mapping from forecast probability to QPF.

2.2.2 OPTIMAL INTEGRATION METHOD

The optimal integration (OPI) method acquires the optimal forecast by integrating the best members in weak and severe precipitation forecasts. The steps are shown in Fig. 3. Firstly, a study area was selected. Among all the multi-method calibrated members, members A and B were assumed to have the optimal performance for weak precipitation and severe precipitation, respectively. Next, all stations in the study area were divided into two groups. The stations where members A or B showed severe precipitation were classified into G1, and the remaining stations were classified into G2. For stations in G1, the OPI model integrated the values of member B. For stations in G2, the OPI integrated the values of member A to obtain the integrated QPF. Finally, a new rule was introduced to avoid the problem of continuous precipitation under long-term statistical conditions. That is, for all severe precipitation stations in the integrated QPF, whether their precipitation grades in members A and B spanned more than two orders was checked. Stations with more than two orders were replaced with the average of members A and B.

Then, a comparative experiment using a shorter sliding training window was conducted (Table 4). Specifically, the OPI experiment used the optimal severe rain member in the whole validation period as member B; the OPI-sliding experiment uses the sliding optimal rainstorm (≥8 mm) member in training window.

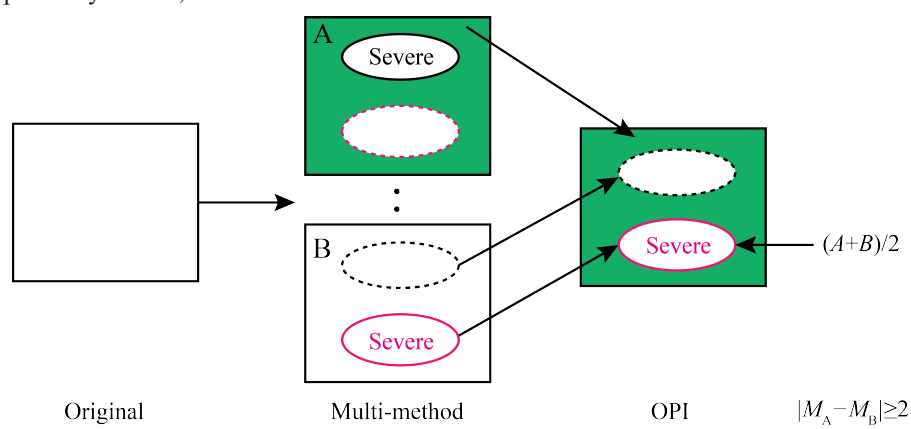

Figure 3. Schematic diagrams of the principles of the OPI method. Assuming that members A and B have the best weak rainfall and severe rainfall among all the multi-method calibrated members, respectively. The balck and red circles represent the severe rainfall stations of A and B, respectively, and the green part represents stations with weak rainfall. M_A and M_B indicate the precipitation magnitude of stations in A and B, respectively.

2.3 *Evaluation method*

Two assessment indicators including threat score (TS) and clear-rainy TS were used to assess the QPF of different bias-corrected methods. Root-mean-square error (RMSE) and mean absolute error (MAE) were used to verify the performance of DNN. Table 5 shows the calculation formulas.

3 RESULTS

3.1 *Results of DNN*

Figure 4a shows the classification accuracy of the DNN model on the training and validation datasets. On the training dataset, the accuracy increases steadily to relative equilibrium with the increase in training epochs. In the validation set, the model has the best effect in about the 30-50th epochs, with an accuracy of more than 76.5%, and the highest point appears in the 44th epoch, which is 77.2%. It is noted that the accuracy of the training set is lower than that of the verification set, which may be related to their sample balance and imbalance (Table 1).

Figure 4b compares the RMSE and MAE in each initial time between CMA-GD and DNN. DNN achieves almost the same performance as CMA-GD, with their difference failing to pass the Wilcoxon rank sum test with a confidence level of 95%, which also demonstrates that the DNN follows the basic physical laws of CMA-GD.

3.2 *Results of OPI*

Comparing the results of the three techniques (DNN, FM and OTS) in the validation set revealed that DNN has an optimal performance for clear-rainy and light rain forecasts, but OTS has the best performances for the other magnitudes of precipitation (Fig. 5). Specifically, in clear-rainy forecasts, DNN (0.869) and FM (0.868) show the highest scores, with

Table 4. Design of the sensitivity experiments.

Experiments	Member of weak rain	Member of severe rain	Training window
OPI	Overall optimum	Overall optimum	The whole period
OPI-sliding	Overall optimum	Sliding optimum	Same as FM

Table 5. Assessment indicators used in the evaluation of QPF. NA, NB, NC, and ND represent the number of hits, misses, false alarms, and correct negatives, respectively. O and F stand for the observations and model results, respectively. i represents the ith sample, and N represents the number of valid samples.

Indicator	Expression
Threat score (TS)	$\frac{\mathrm{NA}}{\mathrm{NA}+\mathrm{NB}+\mathrm{NC}}$
Clear-rainy TS	$\frac{\mathrm{NA}+\mathrm{ND}}{\mathrm{NA}+\mathrm{NB}+\mathrm{NC}+\mathrm{ND}}$
Root-mean-square error (RMSE)	$\sqrt{\frac{1}{N}\sum_{i=1}^{N}(F_i-O_i)^2}$
Mean absolute error (MAE)	$\frac{1}{N}\sum_{i=1}^{N}\lvert F_i-O_i\rvert$

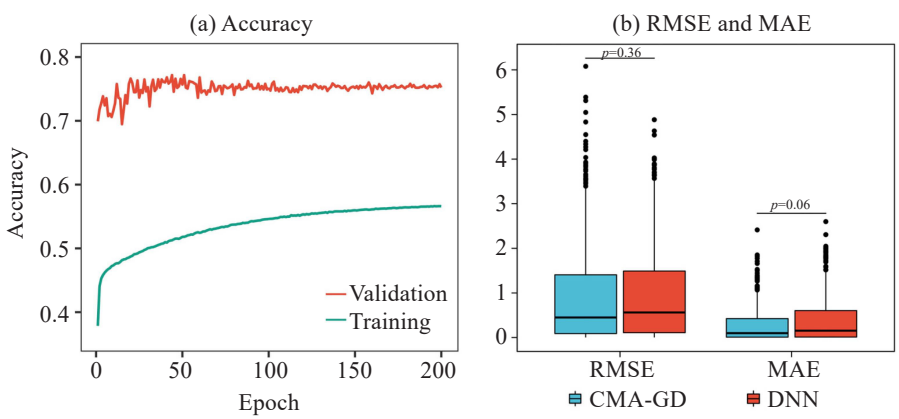

Figure 4. (a) Classification accuracy on the training and validation datasets. (b) Significance test of RMSE and MAE in each initial time in the verification datasets between CMA-GD and DNN.

no noticeable difference. In light rain forecasts, DNN has the highest TS score of 0.374, followed by OTS (0.358) and FM (0.338). From moderate rain to rainstorms, OTS improved TS by 0.6%, 5.6%, and 1.4% compared with CMA-GD.

As a result, DNN and OTS are used as the overall optimal members of weak rain and severe rain in the sensitivity experiments (Table 4). Heavy rain (4 mm) is regarded as the 'weak' and 'severe' dividing line here in OPI (Fig. 2). According to the experimental results, both OPI and OPI-sliding show significant improvements over CMA-GD in weak forecasts. But in severe forecasts, only OPI can enhance the original forecast. Furthermore, OPI realizes improvements of 2.5%, 5.4%, 7.8%, 8.3%, and 6.1% compared with CMA-GD for each magnitude of precipitation and of 2.1%, 5.3%, 7.1%, 2.5%, and 4.7% compared with

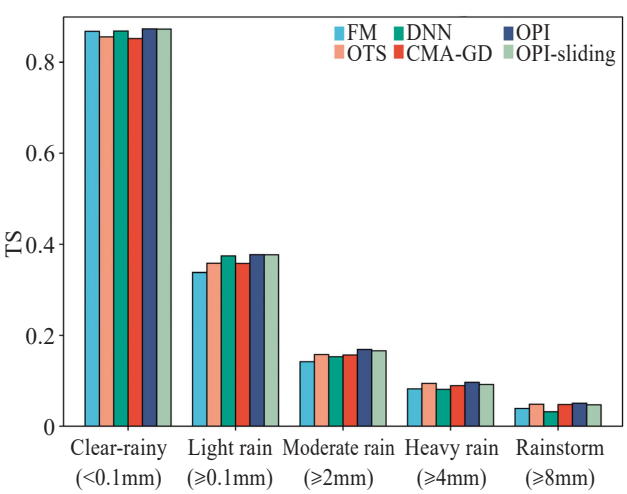

Figure 5. Threat score of multi-method hourly QPF. Details of the method are shown in Table 2 and 4.

OTS.

Figure 6 displays the performance of the OPI method in the 0-24 h forecast periods. Compared with CMA-GD, OPI improves the forecast periods by 100%, 100%, 91.7%, 87.5% and 75% for predictions from clear-rainy to rainstorms, respectively.

In conclusion, OPI can improve QPF for all magnitudes of precipitation simultaneously, and the improvement works at more than 75% of the 0-24 h lead time.

3.3 *Assessment on test data*

To verify the stability of OPI method, it is applied and evaluated on the test set. Overall, three methods can simultaneously improve QPF of CMA-GD in all magnitude: OTS, OPI, and OPI-sliding (Fig. 7a). Additionally, OPI has the best performance, with increases of 3.3%, 4.8%, 6.6%, 6.3%, and 9.9 % for prediction from clear-rainy to rainstorms. From the perspective of the 0-24 h lead time, the results in the test set are consistent with the results on the validation set, improving the forecast periods by 100%, 95.8%, 83.3%, 79.2%, and 75% for predictions from clear-rainy to rainstorms (Fig. 7b). This indicates that OPI has good stability in different datasets.

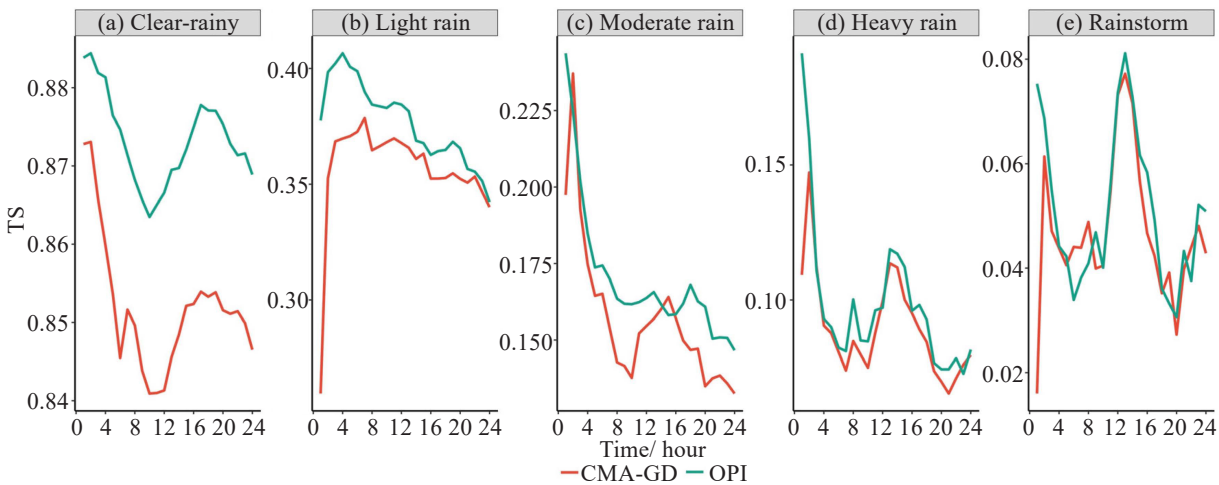

Figure 6. Comparison of hourly TS between CMA-GD and OPI in a lead time of 0-24 h on the validation datasets.

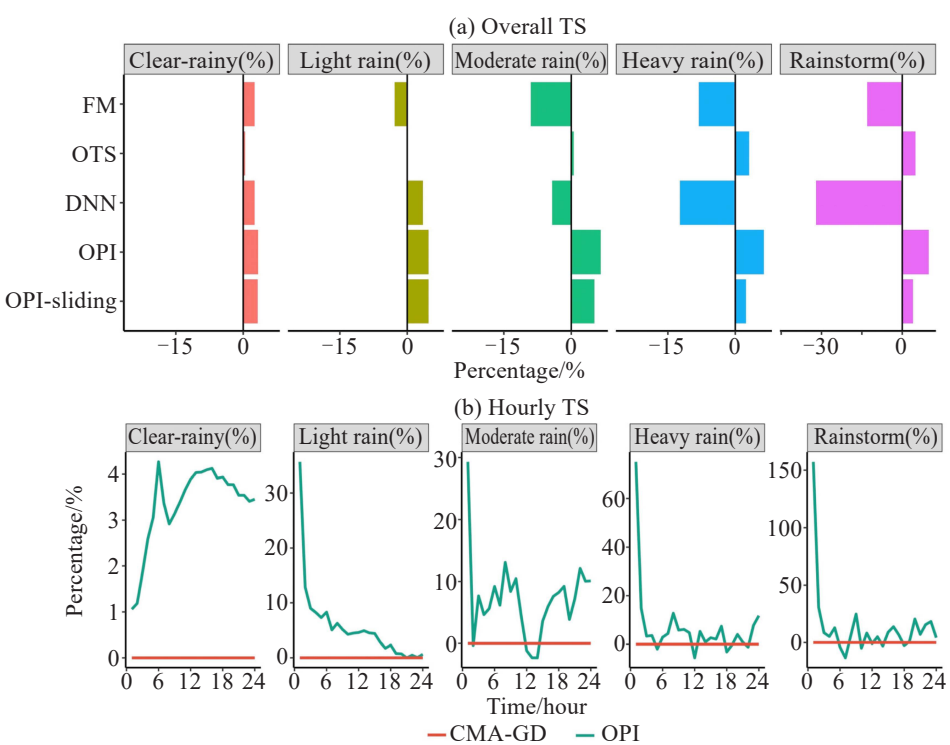

Figure 7. Percentage of TS improvement by different methods on test datasets. (a) Bar chart of overall TS and (b) line chart of hourly TS. Details of the method are shown in Table 2 and 4.

4 CASE STUDY

Advantages and disadvantages of the new approach are discussed here using four cases (Fig. 8).

Advantages: For weak precipitation, CMA-GD shows high false alarms while the OPI method can effectively eliminate false alarms and improve the clear-rainy forecast (Fig. 8c-h). For severe precipitation, OPI can decrease the number of missing rainstorms compared with CMA-GD (Fig. 8b) and the number of false alarms (Fig. 8d, f). For instance, in Case III (Fig. 8f), redundant precipitation of CMA-GD in the northwest of Hunan Province are eliminated by OPI, and the false alarms for heavy rainstorms in the southeast are weakened (≥100 mm). As a result, OPI shows closer rainfall patterns and intensities to those of the observations.

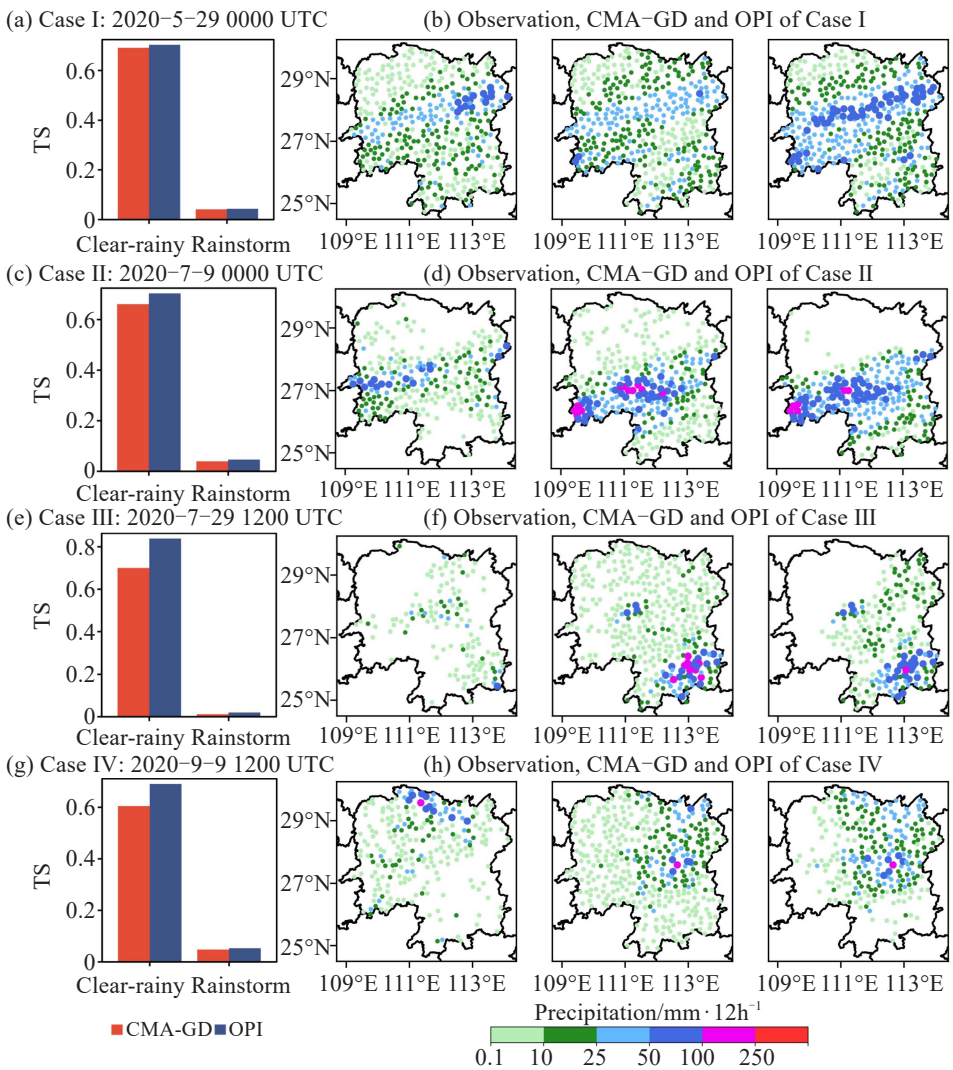

Figure 8. Overall TS (left panels) and 12-hour precipitation distribution of observation, CMA-GD, and OPI (right panels). Initial forecasting time was 00:00 UTC May 29, 00:00 UTC July 9, 12:00 UTC July 29, and 12:00 UTC September 9 in 2020, respectively.

Disadvantages: It is noted that the rainstorm pattern of OPI relies heavily on the original forecast. For example, in Case IV (Fig. 8g-h), CMA-GD mistakenly predicted the rainstorm in the north as being in the south, and OPI cannot correct this deviation in location although the TS increased.

5 CONCLUSIONS

Based on the high-resolution CMA-GD products (3km, hourly) from 2018 to 2021, this paper proposes a simple and powerful approach to improve the QPF of a single model. The following is a summary of the findings:

(1) The QPF of DNN follows the basic laws of CMA-GD. DNN and CMA-GD show almost the same performances as their difference failed to pass the significance test. In addition, DNN has the optimal performance compared with the other two techniques (FM and OTS) in clear-rainy and light rain forecasts, but OTS has the best performances for the other magnitudes of precipitation. As a result, DNN and OTS are used as the overall optimal members of weak

rain and severe rain in the sensitivity experiments.

(2) According to the experiment results, OPI with the overall optimum member is better than OPI-sliding with the sliding optimal member in the verification set. Although both OTS and OPI can improve QPF from clear-rainy to rainstorms simultaneously, OPI is better than OTS. Furthermore, OPI realizes improvements of 2.5%, 5.4%, 7.8%, 8.3%, and 6.1% compared with CMA-GD for each magnitude of precipitation and the improvement works at more than 75% of the 0-24 h forecast period for all magnitudes.

(3) In test dataset, OPI shows good stability. Additionally, OPI still has the best performance for all magnitudes among all techniques, with increases of 3.3%, 4.8%, 6.6%, 6.3%, and 9.9% compared with CMA-GD from clear-rainy to rainstorms. The results are consistent with those in the validation set. In the case study, the new approach can effectively eliminate false alarms of weak precipitation and decrease the number of missing rainstorms and the false alarm.

According to the findings above, the new approach achieves state-of-the-art performances on a single model for all magnitudes of precipitation. In this study, the OPI method based on DNN and OTS can effectively improve the QPF of CMA-GD. DNN can create a predictive model by mining the relationships between physical variables to improve the QPF. However, such an improvement is ineffective for severe precipitation. OTS can help improve severe weather forecasting, and OPI combines their advantages. However, it is mentioned that the rainstorm pattern of OPI relies heavily on the original forecast and that OPI cannot correct for deviations in the location. More research into the severe precipitation issue will be conducted in the future.

REFERENCS

[1] BAUER P, THORPE A, BRUNET G. The quiet revolution of numerical weather prediction [J]. Nature, 2015, 525: 47-55, https://doi.org/10.1038/nature14956.

[2] LEUTBECHER M, LOCK S J, OLLINAHO P, et al. Stochastic representations of model uncertainties at ECMWF: State of the art and future vision [J]. Quarterly Journal of the Royal Meteorological Society, 2017, 143 (707): 2315-2339, https://doi.org/10.1002/qj.3094.

[3] DIAS J, GEHNE M, KILADIS G N, et al. Equatorial waves and the skill of NCEP and ECMWF numerical weather prediction systems [J]. Monthly Weather Review, 2018, 146(6): 1763-1784, https://doi.org/10.1175/MWR-D-17-0362.1.

[4] XUE J S, LIU Y. Numerical weather prediction in China in the new century—Progress, problems and prospects [J]. Advances in Atmospheric Sciences, 2007, 24: 1099-1108, https://doi.org/10.1007/s00376-007-1099-1.

[5] SUBRAMANIAN A, JURICKE S, DUEBEN P, et al. A stochastic representation of subgrid uncertainty for dynamical core development [J]. Bulletin of the American Meteorological Society, 2019, 100(6): 1091-1101, https://doi.org/10.1175/BAMS-D-17-0040.1.

[6] ZHANG Xu-bin, WAN Qi-lin, XUE Ji-shan, et al. The impact of different physical processes and their parameterizations on forecast of a heavy rainfall in south China in annually first raining season [J]. Journal of Tropical Meteorology, 2015, 21(2): 194-210.

[7] BENTZIEN S, FRIEDERICHS P. Generating and calibrating probabilistic quantitative precipitation forecasts from the high-resolution NWP model CosMO-DE [J]. Weather and Forecasting, 2012, 27(4): 998-1002, https://doi.org/10.1175/WAF-D-11-00101.1.

[8] VOLOSCIUK C, MARAUN D, VRAC M, et al. A combined statistical bias correction and stochastic downscaling method for precipitation [J]. Hydrology and Earth System Sciences, 2017, 21(3): 1693-1719, https://doi.org/10.5194/hess-21-1693-2017.

[9] MENDEZ M, MAATHUIS B, HEIN-GRIGGS D, et al. Performance evaluation of bias correction methods for climate change monthly precipitation projections over Costa Rica [J]. Water, 2020, 12(2): 482, https://doi. org / 10.3390/w12020482.

[10] ZHU Yue-Jian, LUO Yan. Precipitation calibration based on the frequency-matching Method [J]. Weather and Forecasting, 2015, 30(5): 1109-1124, https://doi. org / 10.1175/WAF-D-13-00049.1.

[11] HAMILL T M, SCHEUERER M, BATES G T. Analog probabilistic precipitation forecasts using GEFS reforecasts and climatology-calibrated precipitation analyses [J]. Monthly Weather Review, 2015, 143(8): 3300-3309, https://doi.org/10.1175/MWR-D-15-0004.1.

[12] WOODCOCK F, ENGEL C. Operational consensus forecasts [J]. Weather and Forecasting, 2005, 20(1): 101-111, https://doi.org/10.1175/WAF-831.1.

[13] TARTAGLIONE N, MARIANI S, CASAIOLI M, et al. Location errors in QPFs over the Calabria region: Does a multi-model poor man's ensemble over-perform each member? [J]. Atmospheric Research, 2009, 94(4): 736-742, https://doi.org/10.1016/j.atmosres.2009.03.003.

[14] EBERT E E, TURK M, KUSSELSON S J, et al. Ensemble tropical rainfall potential (eTRaP) forecasts [J]. Weather and Forecasting, 2011, 26(2): 213-224, https://doi.org/10.1175/2010WAF2222443.1.

[15] KUMAR A, MITRA A K, BOHRA A K, et al. Multi-model ensemble (MME) prediction of rainfall using neural networks during monsoon season in India [J]. Meteorological Applications, 2012, 19(2): 161-169, https://doi.org/10.1002/met.254.

[16] SUKOVICH E M, RALPH F M, BARTHOLD F E, et al. Extreme quantitative precipitation forecast performance at the Weather Prediction Center from 2001 to 2011 [J]. Weather and Forecasting, 2014, 29(4): 894-911, https://doi.org/10.1175/WAF-D-13-00061.1.

[17] DAI Kan, CAO Yong, QIAN Qi-feng, et al. Situation and tendency of operational technologies in short and medium range weather forecast [J]. Meteorological Monthly (in Chinese), 2016, 42(12): 1445-1455, https://doi. org / 10.7519/j.issn.1000-0526.2016.12.002.

[18] EBERT E E. Ability of a poor man's ensemble to predict the probability and distribution of precipitation [J]. Monthly Weather Review, 2001, 129(10): 2461-2480, https://doi.org/10.1175/1520-0493(2001)1292.0.CO;2

[19] LIU Jin-qing, LI Zi-liang, WANG Qiong-qun.

Quantitative precipitation forecasting using an improved probability-matching method and its application to a typhoon event [J]. Atmosphere, 2021, 12(10): 1346, https://doi.org/10.3390/atmos12101346.

[20] GAGNE D J, MCGOVERN A, XUE M. Machine learning enhancement of storm-scale ensemble probabilistic quantitative precipitation forecasts[J]. Weather and Forecasting, 2014, 29(4): 1024-1043, https://doi. org / 10.1175/WAF-D-13-00108.1.

[21] RASP S, LERCH S. Neural networks for postprocessing ensemble weather forecasts[J]. Monthly Weather Review, 2018, 146(11): 3885-3900, https://doi.org/10.1175/MWR-D-18-0187.1.

[22] HERMAN G R, SCHUMACHER R S. Money doesn't grow on trees, but forecasts do: Forecasting extreme precipitation with random forests [J]. Monthly Weather Review, 2018, 146(5): 1571-1600, https://doi.org/10.1175/MWR-D-17-0250.1.

[23] ZHOU Kang-hui, ZHENG Yong-guang, LI Bo, et al. Forecasting different types of convective weather: a deep learning approach [J]. Journal of Meteorological Research, 2019, 33(5): 797-809, https://doi. org / 10.1007 / s13351-019-8162-6

[24] CHATTOPADHYAY A, NABIZADEH E, HASSANZADEH P. Analog forecasting of extreme-causing weather patterns using deep learning [J]. Journal of Advances in Modeling Earth Systems, 2020, 12(2): e2019MS001958, https://doi.org/10.1029/2019MS001958.

[25] XIA Jiang-jiang, LI Hao-chen, KANG Yan-yan, et al. Machine learning-based weather support for the 2022 Winter Olympics [J]. Advances in Atmospheric Sciences, 2020, 37: 927-932, https://doi. org / 10.1007 / s00376-020-0043-5.

[26] HAN Lei, CHEN Ming-xuan, CHEN Kang-kai, et al. A deep learning method for bias correction of ECMWF 24-240 h forecasts [J]. Advances in Atmospheric Sciences, 2021, 38(9): 1444-1459, https://doi. org / 10.1007 / s00376-021-0215-y.

[27] NAGASELVI M, DEEPA T. Weather forecasting using Deep Feed Forward Neural Network (DFFNN) and fuzzy outlier removal [J]. Journal on Science Engineering & Technology, 2015, 2: 215-225.

[28] REICHSTEIN M, CAMPS-VALLS G, STEVENS B, et al. Deep learning and process understanding for data-driven Earth system science [J]. Nature, 2019, 566(7743): 195-204, https://doi.org/10.1038/s41586-019-0912-1.

[29] CHEN Lei, CAO Yuan, MA Lei-ming, et al. A deep learning-based methodology for precipitation nowcasting with radar [J]. Earth and Space Science, 2020, 7(2): e2019EA000812, https://doi.org/10.1029/2019EA000812.

[30] YUAN Hui-ling, GAO Xiao-gang, MULLEN S L, et al. Calibration of probabilistic quantitative precipitation forecasts with an artificial neural network [J]. Weather and Forecasting, 2007, 22(6): 1287-1303, https://doi. org / 10.1175/2007WAF2006114.1.

[31] SCHER S, MESSORI G. Predicting weather forecast uncertainty with machine learning [J]. Quarterly Journal of the Royal Meteorological Society, 2018, 144(717): 2830-2841, https://doi.org/10.1002/qj.3410.

[32] ZHANG Peng-cheng, CAO Wen-nan, LI Wen-rui. Surface and high-altitude combined rainfall forecasting using convolutional neural network [J]. Peer-to-Peer Networking and Applications, 2021, 14(3): 1765-1777, https://doi.org/10.1007/s12083-020-00938-x.

[33] MARAUN D, SHEPHERD T G, WIDMANN M, et al. Towards process-informed bias correction of climate change simulations [J]. Nature Climate Change, 2017, 7 (11): 764-773, https://doi.org/10.1038/nclimate3418

[34] ZHONG Shui-xin, CHEN Zi-tong, WANG Gang, et al. Improved forecasting of cold air outbreaks over southern China through orographic gravity wave drag parameterization [J]. Journal of Tropical Meteorology, 2016, 22(4): 522-534, https://doi. org / 10.16555 / j. 1006-8775.2016.04.007.

[35] ZHONG Shui-xin, CHEN Zi-tong, XU Dao-sheng, et al. A review on GRAPES-TMM operational model system at Guangzhou Regional Meteorological Center [J]. Journal of Tropical Meteorology, 2020, 26(4): 495-504, https://doi.org/10.46267/j.1006-8775.2020.043.

[36] SUN Chao, HUO qing, REN Zhi-hua, et al. Design and implementation of surface meteorological data statistical processing system [J]. Journal of Applied Meteorological Science (in Chinese), 2018, 29(5): 630-640, https://doi.org/10.11898/1001-7313.20180511.

[37] WU Qi-shu, HAN Mei, LIU Ming, et al. A comparison of optimal-score-based correction algorithms of model precipitation prediction [J]. Journal of Applied Meteorological Science (in Chinese), 2017, 28(3): 306-317, https://doi.org/10.11898/1001-7313.20170305.

[38] WU Ya-li, CHEN De-hui. On use of LHN method to assimilate the intensified surface precipitations for GRAPES_MESO model initialization [J]. Journal of Tropical Meteorology, 2016, 22(4): 544-558, https://doi.org/10.16555/j.1006-8775.2016.04.009.

[39] KINGMA D P, BA J. Adam: A Method for Stochastic Optimization [J]. arXiv preprint arXiv: 1412.6980, 2014.

[40] IOFFE S, SZEGEDY C. Batch normalization: Accelerating deep network training by reducing internal covariate shift [J]. arXiv preprint arXiv: 1502.03167, 2015.

[41] HINTON G E, OSINDERO S, TEH Y W. A fast-learning algorithm for deep belief nets [J]. Neural Computation, 2006, 18(7): 1527-1554, https://doi. org / 10.1162 / neco.2006.18.7.1527.

Citation: LIU Jin-qing, DAI Guang-feng and OU Xiao-feng. An Innovative Bias-Correction Approach to CMA-GD Hourly Quantitative Precipitation Forecasts [J]. Journal of Tropical Meteorology, 2021, 27(4): 428-436, https://doi. org / 10.46267 / j. 1006-8775.2021.037.